Croatian Society for Materials Protection

Metalurgija/Metallurgy

Vol. 65 No. 1 / 2026

Sulfuric Acid Leaching of Zinc Ferrite Residue

Biserka Lucheva[1*], Peter Iliev[1], Nadezhda Kazakova[1], Vladislava Stefanova[1] and Hristo Ivanov[1]

https://doi.org/10.64486/m.65.1.6

[1] Department of Non-Ferrous Metals and Alloys, Faculty of Metallurgy and Materials Science, University of Chemical Technology and Metallurgy, 1756 Sofia, Bulgaria
* Correspondence: plasma@uctm.edu; Tel.: +359887581108

Type of the Paper: Review
Received: August 10, 2025
Accepted: September 10, 2025

Abstract: Zinc ferrite residue, a by-product from the hydrometallurgical processing of zinc calcine, contains significant amounts of zinc, iron, lead, copper, and silver, often locked in complex oxide and spinel phases. This study aims to characterize zinc ferrite residue using ICP-OES analysis, XRD, and SEM/EDS, and to evaluate its behavior during sulfuric acid leaching under controlled laboratory conditions. Thermodynamic modeling with HSC Chemistry software was used to construct Eh–pH diagrams and predict phase stability across different temperatures and redox conditions. The experimental results confirmed efficient leaching of zinc, copper and iron, while lead and silver were largely retained in the insoluble residue. These findings highlight the potential for selective zinc extraction and concentration of lead and silver in the solid phase, offering a promising route for sustainable ZFR processing.

Keywords: zinc ferrite residue, sulfuric acid leaching, thermodynamic modeling

1. Introduction

Zinc ferrite residue (ZFR) is a solid by-product obtained during the acid leaching of zinc calcine, typically accounting for (20–25) % of the mass of the initial zinc concentrate [1]. This residue contains valuable metals such as zinc, iron, lead, copper, and silver, often embedded in complex oxide and spinel phases that are resistant to conventional processing methods.

Pyrometallurgical processes, such as the Waelz process [2], are commonly employed to treat ZFR. However, these methods are highly energy-intensive, produce considerable CO_2 emissions, and result in secondary residues like Waelz clinker, which have limited potential for further processing.

The hydrometallurgical process represents a very promising approach to the effective utilization of this industrial residue. The effectiveness of this method is based on the possibility of recovering copper and silver that cannot be extracted by existing pyrometallurgical schemes.

Hydrometallurgical technologies for ZFR processing can be carried out at atmospheric [3,4,5] and elevated pressure in autoclave [6].

Acidic process schemes can be reductive, where the main objective is the conversion of ferric ions to ferrous ions [7,8], or oxidative, where the aim is to reduce the iron concentration in the production solutions [9]. Alkaline leaching has been used successfully to extract lead and zinc from ZFR [10].

All these schemes have advantages and disadvantages. The choice of process is determined by economic and environmental considerations as well as the chemical and phase composition of the ZFR.

Although zinc ferrite residues have been widely studied by different acid and alkaline leaching approaches, the combined application of thermodynamic modeling and systematic experimental validation under

controlled sulfuric acid conditions has not been thoroughly explored. The aim of the present study is to investigate the elemental and phase composition of ZFR and to evaluate its behavior under sulfuric acid leaching using a combination of experimental techniques (ICP-OES, XRD, SEM/EDS) and thermodynamic modeling with HSC Chemistry software. The study focuses on characterizing the distribution of valuable metals, assessing their selective dissolution under controlled leaching conditions, and integrating experimental results with thermodynamic predictions to better understand phase stability and metal behavior.

2. Materials and Methods

A representative sample of ZFR was kindly provided by the Bulgarian metallurgical company KCM. Prior to characterization, the sample was subjected to water leaching at room temperature for one hour in order to remove water-soluble compounds, mainly zinc sulfate. The insoluble residue was subsequently dried at 105 °C and ground to a particle size of 100 μm using a laboratory knife mill. The content of water-soluble compounds in the ZFR was determined to be 19 %, while 16 % of the zinc was transferred into the solution during water leaching.

Phase analysis of the ZFR was performed by X-ray powder diffraction (XRD) using a Philips PW 1050 diffractometer equipped with Cu-Kα radiation (λ = 1.54185 Å) in the 2θ range of 5°–90°, operated at 40 kV and 30 mA.

The morphology and phase composition of the ZFR were examined by scanning electron microscopy (SEM/FIB LYRA I XMU, TESCAN) at accelerating voltages ranging from 200 V to 30 kV. The instrument was equipped with a tungsten heated filament electron source, providing a resolution of 3.5 nm at 30 kV, and a spectroscopic resolution of 126 eV at Mn-Kα and 1 kcps.

Elemental distribution on the surface of the samples was analyzed using a BRUKER Quantax 200 EDX detector. The bulk chemical composition of both the initial ZFR and the residue obtained after acid leaching was determined by inductively coupled plasma optical emission spectrometry (ICP-OES) analysis.

To determine the type and content of zinc phases present in ZFR and in insoluble residue from acid leaching experiments, a methodology proposed by [11] is used. A similar methodology for determining the phase composition of zinc compounds is used in [12].

The phase composition of zinc, including zinc in the forms of sulfate, oxide, silicate, ferrite, and sulfide, was investigated through chemical analysis by dissolving the samples in various solvents. In each case, a specific solvent was employed to selectively dissolve a single primary phase. After complete dissolution, the leachate was vacuum-filtered. The solid residues from filtration were used for subsequent phase analyses, while the filtrate was analyzed by ICP-OES to determine the elemental content. A comprehensive overview of all analytical procedures is presented in Figure 1.

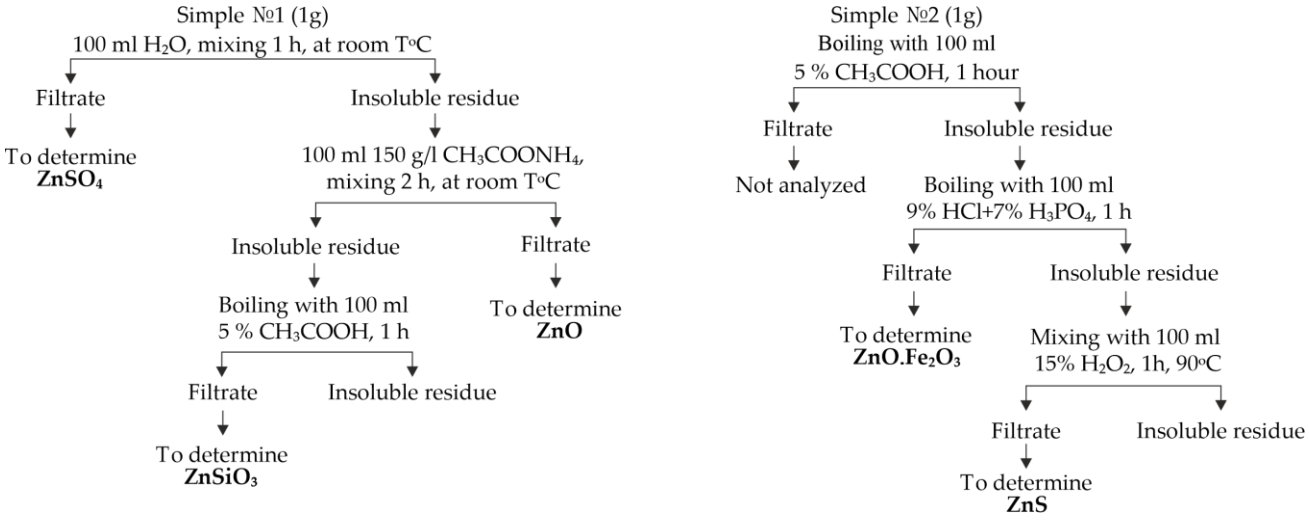

Figure 1. The methodology applied to determine the phase composition of zinc compounds

https://doi.org/10.64486/m.65.1.6

The sulfuric acid leaching of the ZFR was conducted within a glass reactor from Lenz Laborglasinstrumente™, Germany (Figure 2).

Figure 2. Experimental apparatus

The reactor is equipped with a flange, through the central opening of which a stirrer is mounted, and another opening accommodates a jacketed coil condenser. The reactor is connected to a thermostat, allowing experiments to be carried out at controlled temperatures.

For analytical studies, the professional thermochemical software HSC Chemistry (Ver. 10), using the "Reaction Equation" and "Eh–pH Diagrams" modules, was employed.

3. Results and Discussion

3.1. Characterization of ZFR

The elemental composition of the ZFR, determined by ICP-OES, is presented in Table 1. The material is predominantly composed of iron (29.81 %), zinc (18.12 %), and lead (7.43 %), with notable amounts of copper (1.30 %), manganese (1.84 %), and silver (154 g/t), making it a potential source of valuable metals.

Table 1. ZFR elemental composition / mas. %

Zn	Fe	Cu	Pb	Ag	Si	S	Al	Ca	Mn
18.12	29.81	1.30	7.43	0.0154	3.27	3.52	1.11	2.21	1.84

To investigate the mineralogical phases, X-ray diffraction analysis was conducted. The XRD pattern (Figure 3) reveals that the main crystalline phases in ZFR are franklinite ($ZnFe_2O_4$), plumbojarosite, anglesite, and gypsum. Among them, franklinite is the only zinc-bearing phase identified crystallographically, which suggests that a significant portion of zinc is incorporated in a spinel-type structure. This spinel phase is chemically stable and exhibits poor solubility under mildly acidic leaching conditions.

https://doi.org/10.64486/m.65.1.6

The concentration of silver in the residue is below the detection limit of XRD and therefore its crystalline phases could not be identified. Nevertheless, its retention in the solid phase is consistent with the low solubility of Ag in sulfuric acid and the co-precipitation with $PbSO_4$.

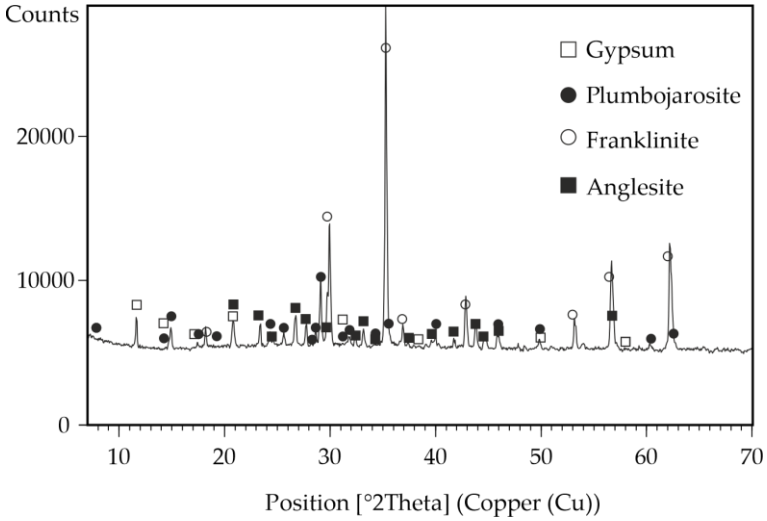

Figure 3. XRD diagram of the ZFR [13]

However, other potential zinc phases—such as ZnO, $ZnSO_4$, Zn_2SiO_4, and ZnS—were not detected by XRD. This may be attributed to their low content, poor crystallinity, or amorphous nature, which are beyond the detection capabilities of this method.

To overcome these limitations and gain a more comprehensive understanding of zinc distribution, a wet chemical phase analysis was performed. The methodology is illustrated in Figure 1, where selective leaching with targeted reagents enables the differentiation of zinc phases. The results of this phase analysis are summarized in Table 2.

Table 2. Phase composition of zinc in ZFR obtained by chemical analysis

Phase	Zinc content in the phase / %	Zinc phase ratio / %
$ZnSO_4$	0.32	1.79
ZnO	0.01	0.08
Zn_2SiO_4	0.52	2.89
$ZnFe_2O_4$	14.12	77.94
ZnS	3.09	17.03
Others	0.05	0.28
Total	18.12	100.00

According to the chemical phase analysis, zinc ferrite accounts for 77.94 % of the total zinc content. Additionally, zinc sulfide (17.03 %) and zinc silicate (2.89 %) are present in significant amounts, while zinc sulfate and zinc oxide contribute minimally. These phases were not detectable by XRD, highlighting the importance of combining both analytical approaches.

The high content of zinc ferrite confirms the refractory nature of the material, limiting zinc recovery through conventional acid leaching. At the same time, the presence of ZnS and Zn_2SiO_4 suggests a heterogeneous phase composition, which may require a combination of redox reactions, complexation, and surface dissolution mechanisms during processing. Understanding this distribution is essential for developing efficient and selective leaching strategies, particularly for recovering zinc from complex secondary resources like ZFR.

The surface morphology of the ZFR sample, illustrated in Figure 4, displays heterogeneous regions varying in color, contrast, and particle size, which reflect the complex phase composition of the residue. To identify the

https://doi.org/10.64486/m.65.1.6

chemical nature of the distinct regions, energy-dispersive X-ray spectroscopy (EDS) was conducted on three representative areas. The corresponding elemental compositions are summarized in Table 3.

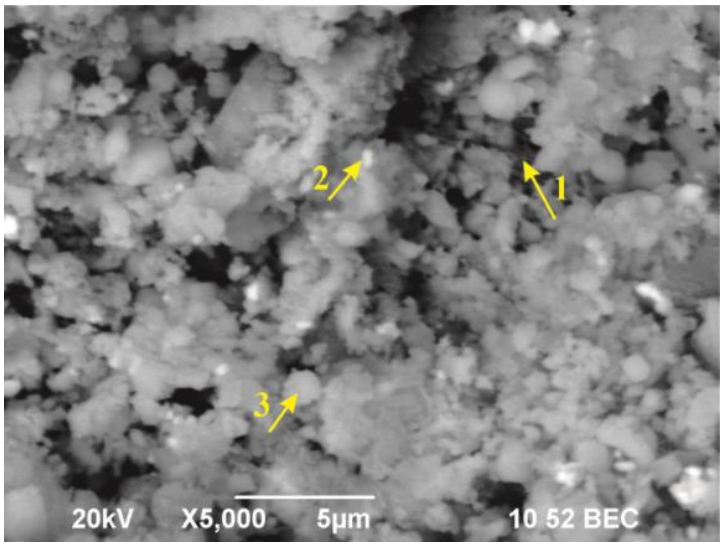

Figure 4. Microstructure of the initial ZFR sample

Table 3. Microanalysis of the more characteristic phases present in ZFR

Element	Chemical composition / mas. %		
	Spectrum 1	Spectrum 2	Spectrum 3
Zn	13.23	2.15	18.19
Fe	6.01	7.02	33.74
Pb	0.90	36.49	7.50
Cu	0.25	0.21	1.92
O	18.17	33.12	26.92
Al	0.15	0.42	0.93
Si	1.31	10.91	4.23
S	24.55	6.42	3.38
Ca	35.25	0.13	1.36
Mn	0.18	2.75	1.83

Spectrum 1, corresponding to dark regions in the micrograph, exhibits high concentrations of calcium (35.25 %) and sulfur (24.55 %), along with notable oxygen content (18.17 %). This composition strongly suggests the presence of gypsum ($CaSO_4 \cdot 2H_2O$) or anhydrite ($CaSO_4$).

Spectrum 2, identified in bright regions of the micrograph, contains elevated levels of lead (36.49 %), oxygen (33.12 %), and sulfur (6.42 %), which is consistent with the presence of plumbojarosite [$PbFe_6(SO_4)_4(OH)_{12}$] or anglesite ($PbSO_4$). The presence of silicon (10.91 %) may also indicate silicate admixtures or inclusions within these phases.

Spectrum 3, representing light grey regions, is characterized by a high content of iron (33.74 %) and zinc (18.19 %), which matches the composition of franklinite ($ZnFe_2O_4$). Trace amounts of copper, manganese, calcium, and silicon were also detected, indicating either solid solution formation or surface interaction with adjacent phases.

These microstructural and compositional observations align with the XRD results (Figure 3) and further confirm the heterogeneous nature of the ZFR, with a mixture of sulfate, oxide, and silicate phases distributed

https://doi.org/10.64486/m.65.1.6

irregularly across the sample. This heterogeneity must be considered in process design, as it influences the leaching behavior and reagent requirements for efficient metal recovery.

3.2. Thermodynamic analysis of the sulfuric acid leaching process of ZFR

The use of sulfuric acid in processing zinc residue is both technologically and economically justified, as it yields a zinc sulfate solution that can be returned to the main cycle of the zinc plant. The choice of sulfuric acid as the solvent is determined by its wide availability at any zinc plant, where it is produced in sufficient quantities during electrolysis and from roasting gases on site.

According to literature sources [14–18], the following chemical reactions may occur during the sulfuric acid leaching of ZFR:

$$ZnFe_2O_4 + 4H_2SO_4 \rightarrow ZnSO_4(a) + Fe_2(SO_4)_3 + 4H_2O \quad (1)$$

$$ZnFe2O_4 + H_2SO_4 \rightarrow ZnSO_4(a) + Fe_2O_3 + H_2O \quad (2)$$

$$Fe_2O_3 + 3H_2SO_4 \rightarrow Fe_2(SO_4)_3 + 3H_2O \quad (3)$$

$$ZnO + H_2SO_4 \rightarrow ZnSO_4(a) + H_2O \quad (4)$$

$$CuO + H_2SO_4 \rightarrow CuSO_4 + H_2O \quad (5)$$

$$Cu_2O + H_2SO_4 \rightarrow Cu_2SO_4 + H_2O \quad (6)$$

$$CuO*Fe_2O_3 + H_2SO_4 \rightarrow CuSO_4 + Fe_2O_3 + H_2O \quad (7)$$

$$Cu_2O*Fe_2O_3 + H_2SO_4 \rightarrow Cu_2SO_4 + Fe_2O_3 + H_2O \quad (8)$$

$$2Pb_{0.5}Fe_3(SO_4)_2(OH)_6 + 6H_2SO_4 \rightarrow PbSO_4 + 3Fe_2(SO_4)_3 + 12H_2O \quad (9)$$

In constructing the Eh–pH diagrams, the molar concentrations of the main components of ZFR (Zn, Pb, and Fe) were calculated in mol/kg H_2O at a solid-to-liquid ratio of 1:10, assuming 200 g/L H_2SO_4 (Table 4).

Table 4. The molar concentrations of the main components present in zinc-ferrite residue in M/kgH_2O.

S:L	Fe	Pb	Zn	S (200g/L H_2SO_4)
1:10	0.534	0.0358	0.277	2.041

The relevant ionic and non-ionic species and their Gibbs free energies used in thermodynamic modeling are provided in Table 5.

Table 5. The Gibbs free energy of the main types of ionic and non-ionic forms of substances in the system Zn-Pb-Fe-S-H_2O

Species	ΔG, kJ/mol		Species	ΔG, kJ/mol	
	T = 50 °C	T = 90 °C		T = 50 °C	T = 90 °C
Zn			**Fe**		
$ZnFe_2O_4$	-1064.924	-1050.849	Fe_2O_3	-737.384	-726.464
ZnS	-198.138	-197.522	Fe_3O_4	-1003.712	-990.014
Zn(+2)	-146.720	-145.804	FeO*OH	-484.574	-475.093
Pb			Fe(+3a)	-14.414	-9.778
$Pb_{0.5}Fe_3(SO_4)_2(OH)_6$	-3076.474	-3008.878	Fe(+2a)	-91.441	-91.220
$PbSO_4$	-804.060	-789.688	**S**		
PbS	-98.583	-98.357	SO_4(-2a)	-730.146	-706.096
Pb(+2)	-26.301	-29.464			

The Eh–pH diagrams for the Zn–Fe–Pb–S–H_2O system at 50 °C and 90 °C are shown in Figure 5. At 50 °C, plumbojarosite coexists with hematite within a pH range of approximately 3.32–4.34 and an oxidation-reduction potential above –0.06 V. As the pH increases to 4.34–5.61, plumbojarosite coexists with zinc ferrite, while at pH values above 5.61, the stability region of zinc ferrite overlaps with that of anglesite.

https://doi.org/10.64486/m.65.1.6

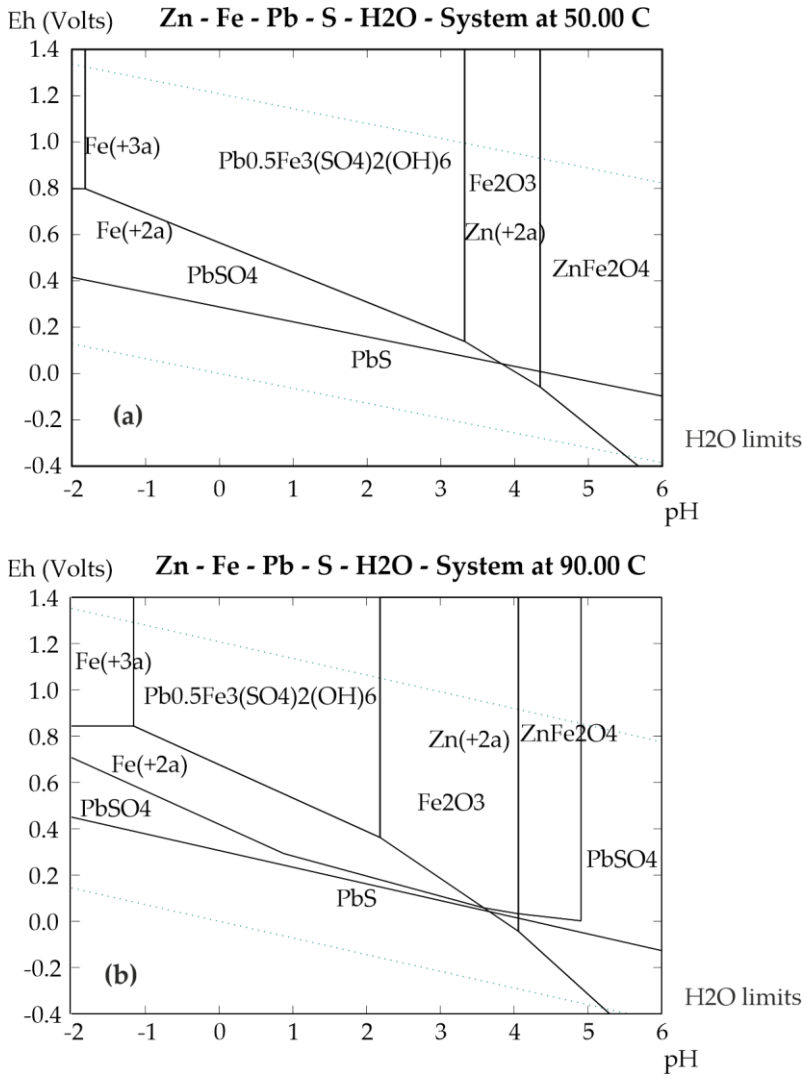

Figure 5. Influence of temperature at solid liquid ratio 1:10 and acid concentration of 200 g/l on the regions of stability of ionic and non-ionic forms of substances in the system Zn-Fe-Pb-S-H_2O
(a) $T = 50$ °C; (b) $T = 90$ °C

Increasing the temperature to 90 °C causes notable changes in phase stability. The hematite region shrinks and shifts toward lower pH values, near 2.18, while the stability region of anglesite expands significantly. In contrast, the regions of zinc ferrite and plumbojarosite contract and shift toward higher potentials, and the Fe^{3+} stability region increases. These results indicate that under 90 °C, 200 g/L H_2SO_4, and a solid-to-liquid ratio of 1:10, the leach solution is likely to contain dissolved zinc and ferrous ions due to jarosite formation, whereas lead is expected to remain predominantly in the solid phase. It should be noted that reaction time, not accounted for in the thermodynamic calculations, may also influence dissolution.

The temperature-dependent changes observed in the Eh–pH diagrams emphasize the critical role of temperature in determining phase stability within the Zn–Fe–Pb–S–H_2O system. The expansion of the hematite and Fe^{3+} stability fields, combined with the contraction of plumbojarosite and zinc ferrite regions, indicates that temperature strongly influences which phases dissolve or remain stable. This insight is valuable for designing leaching conditions that selectively recover zinc while minimizing the dissolution of lead. Moreover, the modeling results provide a predictive tool for controlling redox conditions during industrial leaching operations.

https://doi.org/10.64486/m.65.1.6

Careful control of temperature, *Eh*, pH, reaction time, and reagent addition allows the leaching process to be optimized for maximum zinc recovery, controlled iron behavior, and minimal lead dissolution. Such optimization is essential for achieving both economic efficiency and environmental sustainability in hydrometallurgical operations.

3.3. Sulfuric acid leaching of ZFR

Two parallel sulfuric acid leaching experiments of ZFR were carried out at 90 °C, using a sulfuric acid concentration of 200 g/L, a solid-to-liquid ratio of 1:10, and a leaching time of 5 hours. Under these conditions, sulfuric acid leaching at atmospheric pressure (90 °C, 200 g/L H_2SO_4) achieves a high extraction efficiency of zinc (98.3 %), copper (96.4 %), and iron (92.72 %) from ZFR. The average chemical compositions of the leach products, determined by ICP-OES analysis, are presented in Table 6.

Table 6. Chemical composition of the leaching products

Products	Chemical composition				
	Fe	Zn	Pb	Cu	Ag
Solution / (g/L)	27.64	17.81	-	1.25	-
Insoluble residue / %	7.98	1.13	26.84	0.17	0.0554

The experimental results confirm the predicted behavior of the Zn–Fe–Pb–S–H_2O system, demonstrating close agreement with the Eh–pH diagrams. Zinc and iron were found at high concentrations in the leach solution (17.81 g/L Zn and 27.64 g/L Fe), while copper was almost completely leached (1.25 g/L, >95 % extraction efficiency). These findings indicate good solubility of Zn, Fe, and Cu under the applied acidic conditions, consistent with thermodynamic predictions that Zn^{2+} and Fe^{2+}/Fe^{3+} are stable in solution and copper occurs in readily soluble phases. In contrast, lead and silver largely remained in the solid residue (26.84 % Pb and 0.0554 % Ag), reflecting their low solubility and confirming their presence in insoluble forms such as $PbSO_4$, PbS, or highly stable silver phases.

The leaching conditions investigated are compatible with existing hydrometallurgical infrastructure in zinc plants. The selective dissolution of zinc, copper, and iron, combined with the retention of lead and silver in the residue, provides a solid basis for integrating this process into an industrial flow sheet. Iron can be precipitated as hematite in an autoclave and the solution reused for subsequent leaching cycles, while copper can be removed by cementation and zinc recovered by electrowinning. The insoluble Pb–Ag residue can be further processed through chloride leaching to obtain a lead–silver product [13]. These process options, together with the reuse of leach solutions and the recovery of iron as hematite, align with sustainable and circular economy principles, highlighting the potential for scale-up and implementation in real-world operations.

5. Conclusions

The present study demonstrates that ZFR, a by-product of zinc hydrometallurgy, contains significant amounts of Zn, Fe, Cu, Pb, and Ag, mainly bound in complex oxide and spinel phases. A combined approach of thermodynamic modeling and experimental validation was applied to evaluate its behavior under sulfuric acid leaching.

The results revealed that leaching at 90 °C with 200 g/L H_2SO_4 and a solid-to-liquid ratio of 1:10 enables selective dissolution of zinc, copper, and iron, achieving recoveries of 98.3 % Zn, 96.4 % Cu, and 92.72 % Fe. In contrast, Pb and Ag remained concentrated in the solid residue, in line with theoretical predictions. This demonstrates the potential for a two-step recovery strategy in which base metals are efficiently leached, while the Pb–Ag rich fraction is preserved for subsequent treatment.

Beyond the laboratory scale, the applied conditions are compatible with industrial hydrometallurgical practice, supporting scalability of the process. The ability to selectively recover multiple valuable metals, mini-

https://doi.org/10.64486/m.65.1.6

mize waste, and generate a secondary concentrate enriched in Pb and Ag highlights the economic and environmental benefits of the approach. Therefore, the proposed leaching scheme provides a sustainable and industrially relevant pathway for the utilization of ZFR.

Acknowledgments: This research was funded by European Union Next Generation EU, through the National Recovery and Resilience Plan of the Republic of Bulgaria, project №BG-RRP-2.004-0002, "BiOrgaMCT".

References

[1] Kh. Khaydaraliev, D. Kholikulov, "Research into modern technologies of hydrometallurgical processing of zinc cakes", *Journal of Advances in Engineering Technology*, vol. 1, pp. 42–51, 2023, https://doi:10.24412/2181-1431-2023-1-42-51.

[2] P. Kozlov, *The Waelz Process*, Ore and Metals Publishing House, 2003.

[3] G. Cusano et al., *Best Available Techniques (BAT) Reference Document for the Non-Ferrous Metals Industries*, Publications Office of the EU, 2017, pp. 617–619, https://doi:10.2760/8224.

[4] R. Sinclair, *The Extractive Metallurgy of Zinc*, Australasian Institute of Mining and Metallurgy, 2005.

[5] F. Cardarelli, Materials Handbook, Springer, 2018, pp. 291–293, https://doi:10.1007/978-3-319-38925-7_3.

[6] D. Matsuura, Y. Usami, K. Ichiya, in: Siegmund A., Alam S., Grogan J., Kerney U., Shibata E. (eds.), 9th International Symposium on Lead and Zinc Processing, PbZn 2020, California, TMS, 2020, pp. 865–885, https://doi:10.1007/978-3-030-37070-1.

[7] F. Yangyang et al., "Reductive leaching of indium from zinc-leached residue using galena as reductant", *Minerals Engineering*, vol. 163, 106777, 2021, https://doi:10.1016/j.mineng.2021.106777.

[8] F. Yangyang et al., "Reductive leaching of indium-bearing zinc ferrite in sulfuric acid using sulfur dioxide as a reductant", *Hydrometallurgy*, vol. 186, pp. 192–199, 2019, https://doi:10.1016/j.hydromet.2019.04.020.

[9] R. Alizadeh, "Recovery of zinc from leach residues with minimum iron dissolution using oxidative leaching", *Waste Management & Research*, vol. 29, no. 2, pp. 165–171, 2011, https://doi:10.1177/0734242X10372661.

[10] C. Zang, "Extraction of zinc from zinc ferrites by alkaline leaching: Enhancing recovery by mechanochemical reduction with metallic iron", *Journal of the Southern African Institute of Mining and Metallurgy*, vol. 116, no. 12, pp. 1111–1114, 2016, https://doi.org/10.17159/2411-9717/2016/v116n12a3.

[11] N.A. Filippova, *Phase analysis of ores and products of their processing*, Moscow: Chemistry, 1975.

[12] Mi Li, Bing Peng, Li-yuan Chai, Ning Peng, Xian-de Xie, Huan Yan,"Technological mineralogy and environmental activity of zinc leaching residue from zinc hydrometallurgical process", *Transactions of Nonferrous Metals Society of China*, 23:1480-1488,2013, https://doi:10.1016/S1003-6326(13)62620-5.

[13] P. Iliev, B. Lucheva, N. Kazakova, V. Stefanova, "Recovery of Iron, Silver and Lead from Zinc Ferrite Residue", *Materials*, vol. 18, 3522, 2025, https://doi:10.3390/ma18153522.

[14] P. Vehmaanperä, *Dissolution of Magnetite and Hematite in Acid Mixtures*; Lappeenranta-Lahti University of Technology LUT University Press: Lappeenranta, Finland, 2022.

[15] V. Gontijo, L. Teixeira, V. Ciminelli, The Reactivity of Iron Oxides and Hydroxides during Low-Temperature Sulfation. *Hydrometallurgy* 2020, *197*, 105452. https://doi.org/10.1016/j.hydromet.2020.105452Get rights and content.

[16] C. Gupta, T. Mukherjee, *Hydrometallurgy in Extraction Processes*, Volume II, 1st ed.; CRC Press: Boca Raton, FL, USA, 1990. https://doi.org/10.1201/9780203751404

[17] T. Havlík, B. Souza, A. Bernardes, I. Schneider, A. Miškufová, Hydrometallurgical Processing of Carbon Steel EAF Dust. *J. Hazard. Mater.* 2006, *135*, 311–318. https://doi.org/10.1016/j.jhazmat.2005.11.067

[18] F. Forray, A. Smith, C. Drouet, A. Navrotsky, K. Wright, K. Hudson-Edwards, W. Dubbin, Synthesis, Characterization and Thermochemistry of a Pb-Jarosite. *Geochim. Cosmochim. Acta* 2010, *74*, pp.215–224.. https://doi.org/10.1016/j.gca.2009.09.033